Polymer 50 (2009) 1588–1595

Contents lists available at ScienceDirect

Polymer

journal homepage: www.elsevier.com/locate/polymer

Lamella reorientation in thin films of a symmetric poly(L-lactic acid)-*block*-polystyrene upon crystallization at different temperatures

Jun Fu [a], Yuhan Wei [a], Longjian Xue [a], Bin Luan [b], Caiyuan Pan [b], Binyao Li [a], Yanchun Han [a,*]

[a] State Key Laboratory of Polymer Physics and Chemistry, Changchun Institute of Applied Chemistry, Chinese Academy of Sciences, Changchun 130022, PR China
[b] Department of Polymer Science and Engineering, University of Science and Technology of China, Hefei 230026, PR China

ARTICLE INFO

Article history:
Received 21 July 2008
Received in revised form
13 January 2009
Accepted 17 January 2009
Available online 9 February 2009

Keywords:
Block copolymer
Crystallization
Thin films

ABSTRACT

The thin films of a symmetric crystalline-coil diblock copolymer of poly(L-lactic acid) and polystyrene (PLLA-*b*-PS) formed lamellae parallel to the substrate surface in melt. When annealed at temperatures well above the glass transition temperature of PLLA block (T_g^{PLLA}), the PLLA chains started to crystallize, leading to reorientation of lamellae. Such reorientation behavior exhibited dependence on the correlation between the crystallization temperature (T_c), the glass transition temperature of PS (T_g^{PS}), the peak melting point of PLLA crystals (T_m^{PLLA}), and the end melting point of PLLA crystals ($T_{m,end}^{PLLA}$). When annealed at (T_c=) 80 °C ($T_c < T_g^{PS} < T_{ODT}$, order–disorder transition temperature), 123 °C ($T_g^{PS} < T_c < T_m^{PLLA} < T_{ODT}$), 165 °C ($T_g^{PS} < T_m^{PLLA} < T_c < T_{m,end}^{PLLA} < T_{ODT}$), the parallel lamellae became perpendicular to the substrate surface, exclusively starting at the edge of surface relief patterns. Meanwhile, the corresponding lamellar spacing was significantly enhanced. The PLLA crystallization between PS layers was hypothesized to account for the lamella reorientation during annealing. The crystallization, chain conformation, and possible chain folding mechanisms were discussed, based on detailed analysis of the lamellar structure before and after crystallization.

1. Introduction

Block copolymers composed of incompatible blocks are known to form segregated phases when cooled down from melt to well below the order–disorder transition temperature, T_{ODT}. Diblock copolymers, for example, have been theoretically and experimentally demonstrated to form body-centered cubic (BCC) spheres, hexagonal cylinders (HEX), gyroids (G), and alternating lamellae (LAM) at $T < T_{ODT}$, depending on the volume fraction of one block [1–4]. These microphase-separated (MPS) structures are at nanometer scale (10–100 nm) as defined by the dimension of polymer chains. In thin films, the orientation of these nanostructures is highly affected by the free surface and the polymer/substrate interface and can be controlled by using proper external fields [5,6].

As one of the blocks is able to crystallize, the interplay of microphase separation and polymer crystallization has been of great research interest. Numerous studies have demonstrated that the crystallization kinetics [7–13], dynamics [13], chain folding [14–17], stem orientation [18–22], and the morphology [8,9,23–32] of the MPS structures are dependent on the correlation of T_{ODT}, the crystallization temperature (T_c), the glass transition temperature of the amorphous component (T_g^a), the thermal history of copolymers, and side chains [33]. Although controversial results have occasionally been reported, some consensus has been widely accepted: crystallization at $T_c < T_g^a < T_{ODT}$ is strictly constrained by the glassy phase; for highly incompatible systems, crystallization can also be strictly confined in the mesophase even though the amorphous component is rubbery ($T_g^a < T_c \ll T_{ODT}$). Loo and coworkers [23] explored the regimes of the interaction between crystallization and MPS structures. They concluded that the crystallization could be confined in, templated by, or break out the microphase-separated structures, depending on the relation of the segregation strength at T_c (i.e., $(\chi N)_c$) and that at T_{ODT} (i.e., $(\chi N)_{ODT}$), where χ is the Flory–Huggins interaction parameter between the blocks and N is the total average degree of polymerization of the copolymers. For poly(high-1,4-butadiene)-*block*-poly(styrene-*r*-butadiene) (E/SEB) diblock copolymers, crystallization in the E spheres was confined by the rubbery SEB at $(\chi N)_c/(\chi N)_{ODT} > 3$, or it broke out the spheres at $(\chi N)_c/(\chi N)_{ODT} < 3$. For E cylinders at $1.5 < (\chi N)_c/(\chi N)_{ODT} < 4$, the crystallization showed sigmoidal kinetics, without completely destroying the mesophases [23]. Similar conclusions were also drawn by Xu et al., according to experiments on isothermal crystallization of poly(oxyethylene) in poly(oxyethylene-*block*-poly(oxybutylene))/poly(oxybutylene) (EB/B)blends [26,27].

* Corresponding author. Tel.: +86 431 85262175; fax: +86 431 85262126.
E-mail address: ychan@ciac.jl.cn (Y. Han).

0032-3861/$ – see front matter © 2009 Elsevier Ltd. All rights reserved.
doi:10.1016/j.polymer.2009.01.048

In thin films, symmetric diblock copolymers form relief structures (holes, bicontinuous pattern, or islands) at the free surface at $T_g < T < T_{ODT}$, as a result of quantization of film thickness by lamellar spacing (L_0) [5,34,35]. Polymer crystallization in block copolymer thin films has been investigated by several groups, primarily focusing on block copolymers in strong segregation limit (i.e., $T \ll T_{ODT}$). Both lamellar spacing and orientation can change upon the folding and unfolding of polymer chains [35–41]. Optiz et al. [36] investigated the confined crystallization of poly(ethylene oxide) in lamellar films of poly(ethylene oxide)–polybutadiene (PEO–PB_h). The lamellar spacing (L_0) was increased as the film was cooled down from melt and a further increase in L_0 was induced upon PEO crystallization: the copolymer chains were stretched due to the decreasing volume (increasing density) of PEO phase. TEM experiments by Hong et al. demonstrated that the PEO chains were oriented along the normal of the PEO/PBD lamellar interface [37]. It was further pointed out that the PEO layers separated by the 10-nm amorphous PBD layers could be in orientational registry at the edge of the dislocation of the lamellar structures. On the other hand, Reiter and coworkers reported a crystallization-induced decrease in the lamellar spacing of a PEO–PB_h thin film, which led to vertical orientation of lamellae with respect to the substrate and free surface [38,39]. Such vertical lamellae could be aligned along the three-phase contact line [38]. Increasing the crystallization temperature could increase the lamellar spacing and finally lead to a transition from perpendicular to parallel orientation of the lamellae with respect to the substrate even at an undercooling of 9° [39]. Recently, PEO crystallization was reported to dominate the formation of lamellar morphologies for grafted PB–PEO diblock copolymers [33]. For weakly segregated PS–PCL (polystyrene–poly(ε-caprolactone)) thin films, Zhang and coworkers reported that PCL crystallization was nucleated at the edge of the relief structures, presumably due to the geometry confinement of fluid flow at the edge [42]. At long time crystallization, the PCL lamellae started to break out the PS layer, probably due to the low T_g of the short PS chains [43].

Previously, we reported the dynamics and kinetics of the interplaying crystallization and microphase separation in the thin films of a symmetric PLLA-*b*-PS [44,45]. When annealed above the PLLA melting point, all the thin films formed layered structures with PS as the top layer and PLLA at bottom. In this paper, we investigate the effect of crystallization of poly(L-lactic acid) on the relief structures of the PLLA-*b*-PS thin films. Due to the unique broad window between the glass transition temperature of PS (T_g^{PS}) and the peak melting point of PLLA (T_m^{PLLA}), it will be interesting to investigate the crystallization within the PLLA-*b*-PS lamellae at different temperatures with respect to T_g^{PS} and T_m^{PLLA}. Within well-established lamellae, the effect of PS layers on the PLLA crystallization depends on the state of the PS phase since the PS and PLLA segregation strength is intermediate according to the theoretical criterion [2]. On the other hand, the isothermal crystallization of PLLA chains induced transitions from parallel to perpendicular lamellae, depending on the crystallization temperatures ($T_c < T_g^{PS}$, $T_g^{PS} < T_c < T_m^{PLLA}$, and $T_m^{PLLA} < T_c < T_{m,end}^{PLLA}$).

2. Experiments

2.1. Materials

The block copolymer of poly(L-lactic acid) and polystyrene (PLLA-*b*-PS) was synthesized by sequential atom transfer radical polymerization (ATRP) of styrene monomers and ring opening polymerization (ROP) of L-lactide [46]. The copolymer had a number average molecular weight ($\overline{M_n}$) of 19,800 ($PLLA_{130}$-*b*-PS_{100}, where the subscripts denote the degree of polymerization) by ^1H NMR and a molecular weight distribution less than 1.2 by gel permeation chromatography (GPC, Waters-150C). The volume fraction of PLLA block is 0.42 and that of PS is 0.58. That is, this copolymer is approximately symmetric.

The thermal behavior of this copolymer was characterized by differential scanning calorimetry (DSC, Perkin–Elmer Diamond Differential Scanning Calorimeter) at 10 °C/min. The PLLA and PS blocks had glass transitions at 55 (T_g^{PLLA}) and 90 °C (T_g^{PS}), respectively. The melting process of PLLA crystals started at 145 °C, reached a peak at 155 °C and finally ended at ($T_{m,end}^{PLLA}$=) 169 °C [47].

It was reported that the Flory–Huggins interaction parameter of PLA (poly(lactic acid)) and PS follows $\chi(T) = 98.1/T - 0.112$, where T is Kelvin temperature [48]. Assuming that the Flory–Huggins interaction parameter between PLLA and PS approximately follows the same equation, one can estimate the segregation strength of PLLA-*b*-PS at specific experimental temperatures [45].

2.2. Sample preparation

The PLLA-*b*-PS powders were dissolved in tetrahydrofuran (THF), a non-selective solvent [47]. After storage for at least 24 h at room temperature, the solutions were spin coated onto freshly cleaned silicon wafers with native oxide surface layer. The silicon wafers used in this study were boiled in a mixture of 98% H_2SO_4 and 30% H_2O_2 (volume ratio 2:1), followed by a thorough rinsing with de-ionized water. The freshly cleaned silicon wafer surface is rich in hydroxyl group and very hydrophilic (water-contact angle 13.55°, glycerol contact angle 15°, surface tension ~71.3 mN/m). The spin coated films were stored in vacuum oven at 40 °C for at least 72 h in order to remove the residual solvent. The film thickness was determined by X-ray reflectometer (Bruker, D8 XRR at 40 kV, 40 mA) or by scanning the edge of the scratches on the films with atomic force microscope. Both methods provided identical results within experimental error. The film thickness was controlled by adjusting the solution concentration.

In order to obtain microphase-separated equilibrium structure, the films were melted in vacuum at 180 °C overnight and then quenched to room temperature [45]. The surface morphologies of the films with different initial thicknesses (h_i) were imaged using tapping mode atomic force microscopy (AFM). Both height and phase images were recorded. Afterward, these microphase-separated films were heated in a convection oven from room temperature to 80 and 123 °C (at an approximate rate of ~5 °C/min) and held at these temperatures for different durations for isothermal crystallization. For AFM investigation, these films were cooled to room temperature and taken out of the oven. Further, these crystallized films were heated again from room temperature to 165 °C which is above T_m^{PLLA} but below $T_{m,end}^{PLLA}$. Such a small overcooling may allow the pre-existing PLLA crystals to readjust their size and shape. These samples were also imaged by tapping mode AFM.

2.3. Tapping mode atomic force microscopy (AFM)

The samples were imaged with a commercial scanning probe microscope (SPM, SPA 300HV/SPI 3800N, Seiko Instrument Inc., Japan) in tapping mode. The sample was driven by a piezo tube scanner in x, y, and z directions (maximum scan area $150 \times 150\ \mu m^2$). A silicon cantilever (nominal spring constant ~2 N/m and resonant frequency ~70 kHz) with an etched tip (radius of curvature ~20 nm) at the free end was used. The set-point was 0.7–0.8 in order to obtain high-quality height and phase images simultaneously. The scan rate was 1.0–2.0 Hz, depending on

the scan area. All the images were analyzed using the software provided by the SPM manufacturer.

3. Results

The orientation of the PLLA-*b*-PS chains after melting and microphase separation at 180 °C were investigated by using X-ray photoelectron spectroscopy, atomic force microscopy, and water-contact angle measurements [45]. The results indicated that the PLLA blocks segregated to the substrate and the interior of the films while the PS blocks segregate to the free surface, forming equilibrium [49] lamellae parallel to the substrate, which constitutes an antisymmetric boundary condition. That is, stable films have a thickness of $(n+1/2)\ L_0$. Otherwise, the films will form relief patterns at the free surface [5,45]. We emphasize that the melting and annealing at 180 °C did not induce film rupture or dewetting, probably due to the pinning of the PLLA chains to the highly polar silicon wafer surface.

Fig. 1 shows the islands and holes formed at the surface of 36 and 26 nm films, respectively. By scratching and scanning the films, we observed a ~10 nm sublayer under the relief structures (Fig. 1c). The relative height of the islands and holes is ~20 nm with respect to the sublayer, indicating the lamellar spacing (L_0). The root mean square roughness (RMS) (based on a $30 \times 30\ \mu m^2$ area hereafter) was 7.7 nm for the 36 nm film and 8.1 nm for the 26 nm film. We compared the film surface morphologies (AFM) in melt and at room temperature. There were no remarkable morphological differences: no perpendicular lamellae were observed; the heights of the surface relief patterns were identical at room temperature and 180 °C.

Then we crystallized PLLA in these parallel PLLA-*b*-PS lamellae at temperatures above T_g^{PLLA} but below $T_{m,end}^{PLLA}$. As the crystallization temperature (T_c) was below T_g^{PS}, one encountered hard confinement from the glassy PS walls; as the crystallization occurred at $T_g^{PS} < T_c < T_{m,end}^{PLLA}$, the rubbery PS phase had a soft confinement on the crystallization. Our concern is how the PLLA crystallization at different temperatures affects the orientation and structure of the parallel PLLA-*b*-PS lamellae in thin films.

First, we crystallized the microphase-separated thin films at 80 °C for 33 h; the surface relief patterns almost remained unchanged, except that bumps appeared at the edge of the islands (Fig. 2 inset) and holes (not shown). The relative height of the islands remained 20 nm, while the RMS slightly changed to 8.0 nm for the 36 nm film and 8.7 nm for the 26 nm film. Remarkably, these bumps contained lamellar structures perpendicular to the surface, as arrowed in Fig. 2. According to the phase image, the perpendicular lamella thickness was ~10 nm in average, very close to the thickness of a single PLLA layer or $L_0/2$. The phase contrast reflects the crystallized PLLA (dark) and soft amorphous PS (light) phases [45,50]. The low phase contrast (2°, Fig. 2b) presumably implied that the PLLA crystallization within these perpendicular lamellae did not break out the PS walls. Similar perpendicular lamellae were also observed at the edge of holes after crystallization at 80 °C for 33 h, with the relative depth of the holes remaining ~20 nm.

As the microphase-separated thin films were crystallized at 123 °C, or $T_g^{PS} < T_c < T_m^{PLLA}$, for 28.5 h, the films ruptured, as shown in Fig. 3. The average height of relief structures was slightly increased from ~20 nm before crystallization to ~24 nm after crystallization. According to the AFM image at the edge of a scratch, the underlayer was cracked and the substrate was exposed to air, as arrowed in Fig. 3c. The cracked underlayer had a height of about 13 nm in average, larger than the original 10 nm ($L_0/2$). The film rupture led to an increase in the surface RMS to 8.2 nm for the 36 nm film and 9.4 nm for the 26 nm film.

Fig. 4 displays typical topography and phase images at the edge of an island. Perpendicular lamellae were apparent, especially in the phase image with alternating dark (crystalline) and bright (amorphous) layers. The lamella thickness had a broad distribution from about 18 nm to about 25 nm, which was much larger than the thickness of PLLA lamellae before crystallization. In addition, the dark PLLA domains were heterogeneous in phase contrast, suggesting that the crystalline domains contained crystals with different degrees of crystallization (Fig. 4b).

The increase in lamellar spacing implies the PLLA chain unfolding [15,16] between the rubbery PS layers at 123 °C. The formation of defects within the PLLA domains suggests the difficulty in chain folding and unfolding due to the entropy penalty arisen from the ordering of the PLLA chains and the repulsion and stretching of the PS chains. At 123 °C, or 33 °C above T_g^{PS}, the rubbery PS chains still have limited mobility and thus constrain the adjustment of PLLA chains.

Such constrains can be relaxed by elevating the crystallization temperature up to at least 50 °C above the T_g^{PS} (when the PS chains are normally known as melt). As the microphase-separated PLLA-*b*-PS films were isothermally crystallized at 165 °C for 24 h, which is between T_m^{PLLA} and $T_{m,end}^{PLLA}$, PLLA crystals did not melt. Instead, the crystals became free of defects and the films were more severely cracked. Fig. 5a shows that the islands almost lose their shape and it is hard to tell the boundary of the islands from the surroundings. The corresponding cross-section profile exhibited a peak-to-valley height of more than 60 nm, which was larger than the absolute

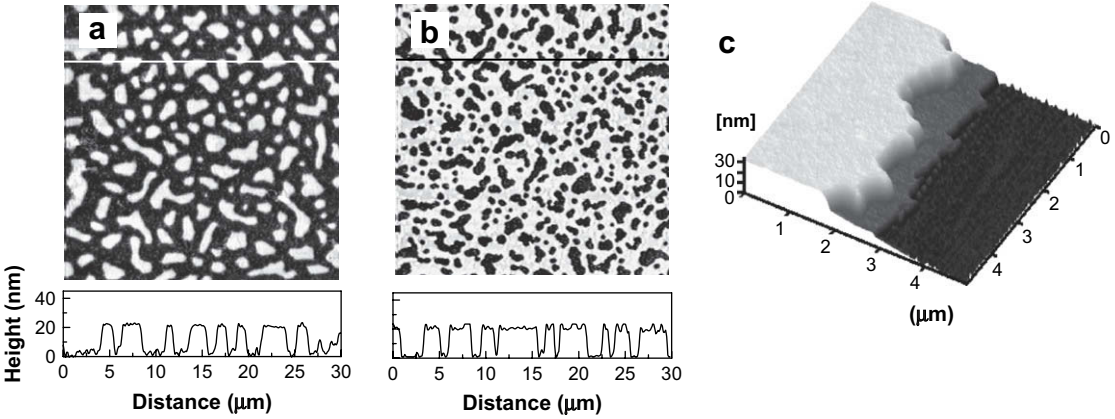

Fig. 1. AFM height images of PLLA-*b*-PS thin films after annealing at 180 °C. The initial film thicknesses were (a) 36, and (b) 26 nm. The corresponding cross-section line scan profiles indicate a lamellar period of 20 nm. A 10-nm sublayer is observed at the edge of a scratch (c).

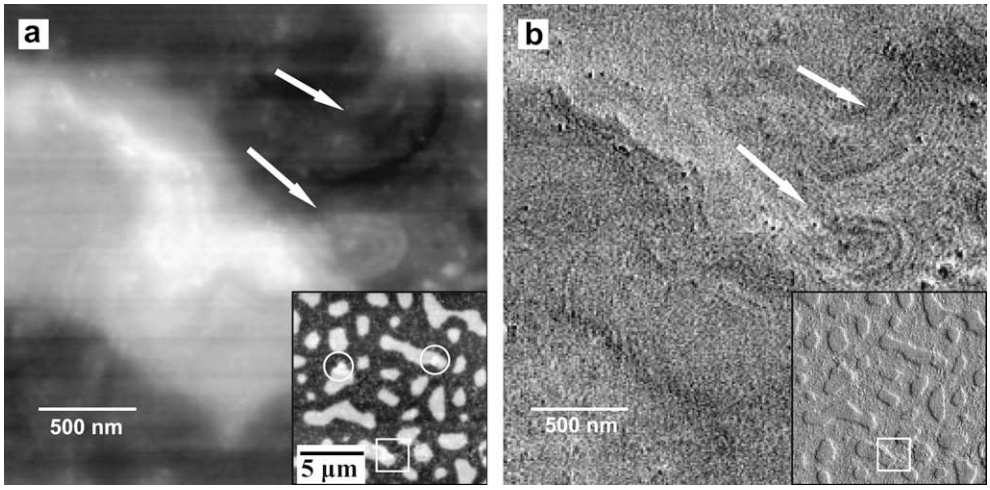

Fig. 2. AFM height (a) and phase (b) images of the microphase-separated 36-nm film after crystallization at 80 °C for 33 h. The insets show a 15 × 15 μm^2 area including the area shown in the main panel. The phase contrast is 2°.

height of the islands relative to the substrate. Similarly, the 26-nm film also cracked after crystallization at 165 °C for 24 h. Both the relief domain and the underlayer contracted so that the area of the relief structure decreased and more of the substrate were exposed to air (Fig. 5b). The cross-section profile indicated that the relative height of the holes with respect to the sublayer was increased to more than 25 nm while the relative height of the sublayer with respect to the substrate was increased to ~13 nm. The overall effects of the cracking and the increases in lamellar thickness led to an increase in the surface RMS to 10.2 and 11.8 nm for the 36 and 26 nm films, respectively.

Fig. 6 displays typical AFM height and phase images of the islands and holes in higher magnification: perpendicular lamellar structures are prevailing. These lamellae were well developed, in comparison to those shown in Figs. 2 and 4. The crystal domain thickness was ~18–25 nm. Moreover, the crystal domains became homogeneous and continuous, constituting well-defined alternating lamellae with light PS layer and dark PLLA crystal layer without defects seen in Fig. 4.

Previously, we reported that most of the small PLLA crystals melted at 155 °C (T_m^{PLLA}), while the large ones may survive until the temperature was as high as 169 °C [44]. A recent study reported that PLLA homopolymer preferably formed edge-on crystals at 165 °C in thin films [51]. In our case, however, the PLLA crystallization was confined by the rubbery PS layers and induced the transformation from parallel to perpendicular lamellae. The perpendicular lamellae appeared as random curves, which are typical for the lamellar structures for symmetric diblock copolymers in bulk and thin films [1]. The conformation of the PLLA crystals will be discussed in the Discussion section. Under the confinement by the PS layers, however, local readjustment of crystal structures may be possible, which is presumably featured by the chain unfolding in small crystals and refolding into larger ones. Thus, the crystal structures were improved via the melting–recrystallizing process at $T_m^{PLLA} < T_c < T_{m,end}^{PLLA}$.

4. Discussion

The polymer chain folding in microphase-separated nanostructures has strong dependence on the crystallization temperature (T_c). As T_c is below the glass transition temperature of the amorphous phase (T_g^a), the polymer chains may have large fold number to avoid a significant stress increase in the crystalline (as well as the amorphous) domain [18]. In fact, the crystal stems may adopt a tilt conformation due to the density decrease induced by crystallization [19]. As T_c is increased to well above T_g^a, the polymer chains gain mobility that permits the adjustment of chain conformation. As a result, the crystalline chains may reduce the fold number, (thus) increase the stem thickness, and probably adopt an orientation perpendicular to the interface of the two phases [15,16].

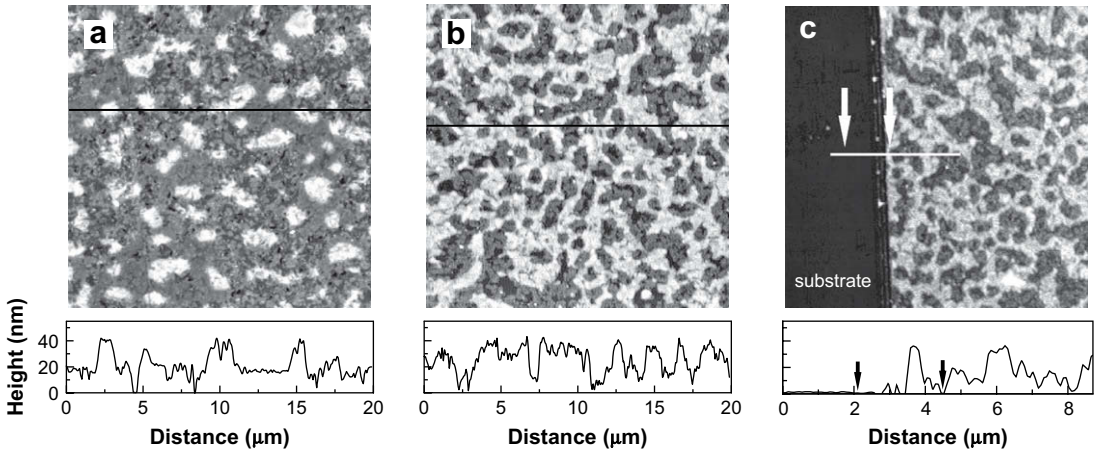

Fig. 3. AFM height images of the microphase-separated 36-nm (a) and 26-nm (b, c) PLLA-*b*-PS films crystallized at 123 °C for 28.5 h. (c) An AFM image at a scratch.

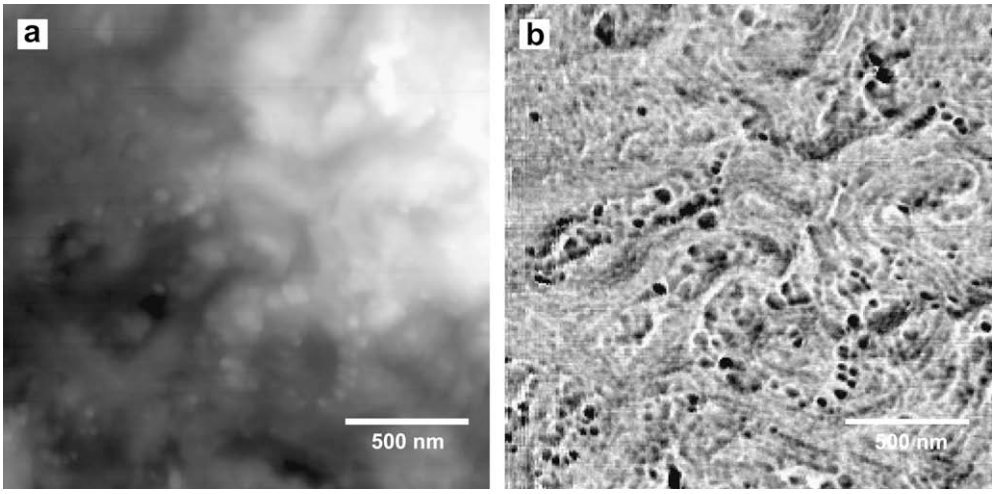

Fig. 4. AFM height (a) and phase (b) images of a $2 \times 2\ \mu m^2$ area at the edge of an island on the 36-nm film after crystallization at 123 °C for 28.5 h. The phase contrast in (b) is 6°.

In our case, PLLA crystallization at 80 °C is strictly constrained between the glassy PS layers. The PLLA chain folding and volume contraction of the PLLA phase may induce internal stress. In bulk, such internal stress could probably induce a corrugated structure [9]. In thin films, however, dislocations are prevailing at the edge of the surface relief patterns [52]. These dislocations, as well as the excess chain stretching therein, may serve as nucleation agents for crystallization [42] and permit break out of PLLA crystals. Thus, we

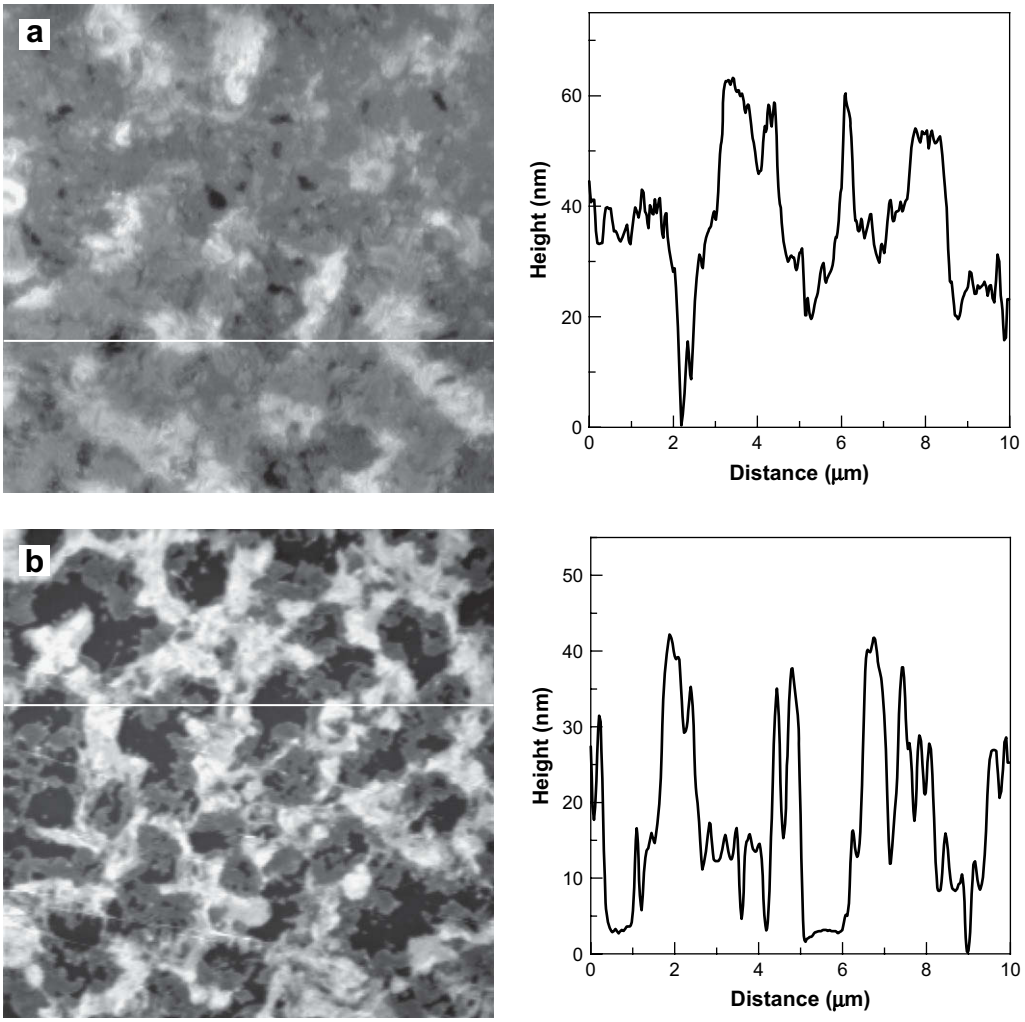

Fig. 5. AFM height images of the 36-nm (a) and 26-nm (b) PLLA-*b*-PS films crystallized at 165 °C for 24 h. The right column displays the corresponding cross-section line scan profiles along the white lines in the images, respectively.

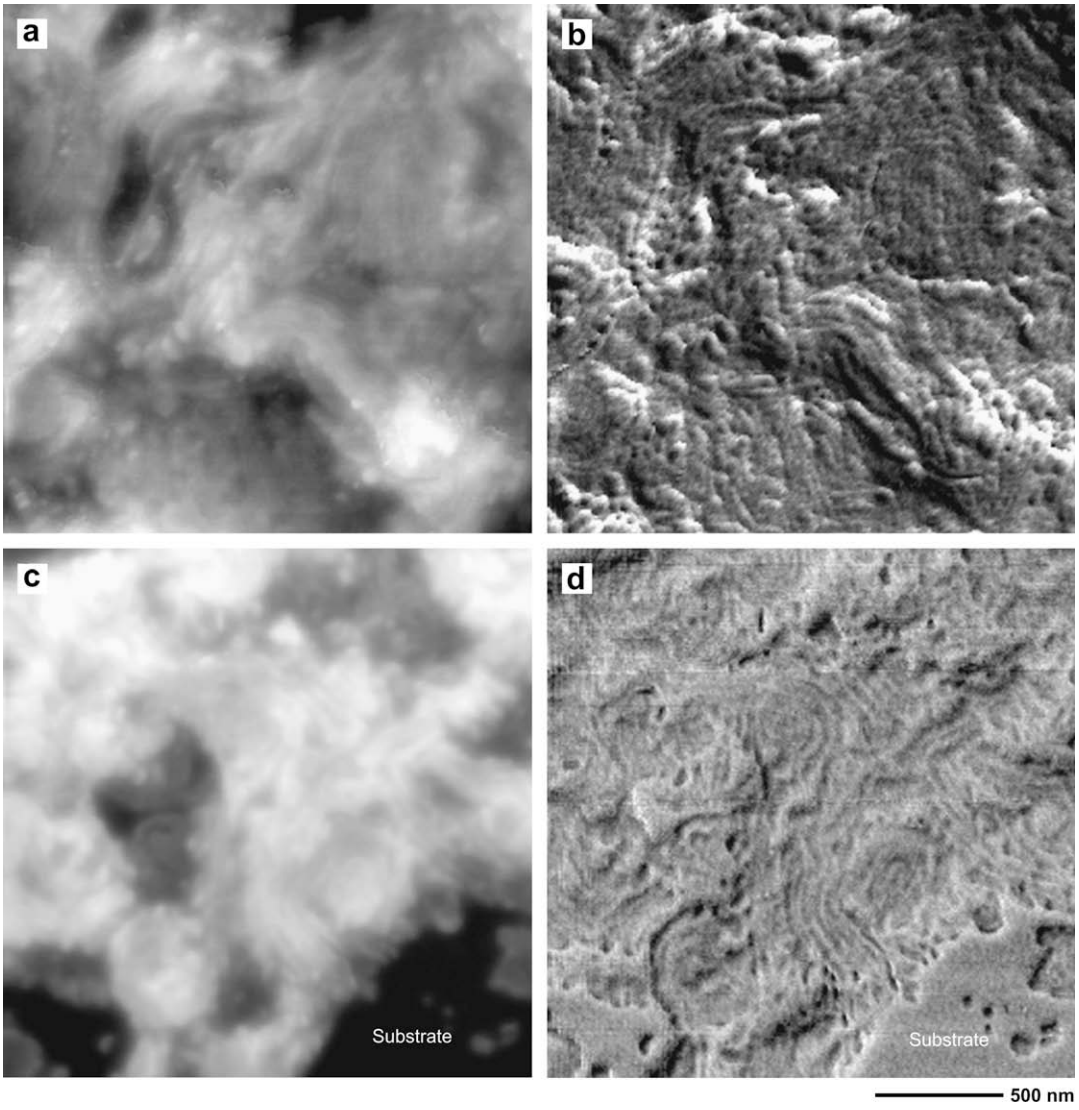

Fig. 6. AFM height (a, c) and phase (b, d) images of the 36-nm (a, b) and 26-nm (c, d) films. The phase contrast is 10°.

observed a large number of crystals at the edge of islands and holes after crystallization at 80 °C for 33 h (Fig. 2). However, the strong constraint from the glassy PS lamellae prohibits further growth of PLLA crystals at prolonged annealing.

As the temperature was increased to above T_g^{PS}, the PLLA chains could reduce fold number and thus increase the stem thickness [16,19]. As a result, the interface between the PS and PLLA chains contracts, which induces an increase in the repulsion between the PS chains. Therefore, the PS chains have to adopt a more stretched conformation, leading to much entropy penalty in the system. Perpendicular lamellae may be favorable because this conformation allows the PS chains to relax (Fig. 7b).

At 123 °C, the rubbery PS phase has a soft confinement on PLLA crystallization and therefore a large number of PLLA nucleation and crystal growth may take place. The stem size is controlled by the lateral diffusion [53] and folding of PLLA chains. Due to the gained PS chain mobility, the PLLA chains start to unfold, which increases the lamellar spacing. Moreover, the increase in the density and spacing of PLLA lamellae induced film rupture (Figs. 3 and 4). However, the PS chains at 123 °C or 33 °C above T_g^{PS} is still not free enough and thus somewhat limit the PLLA chain motion (normally, polymer chains are regarded as melt at a temperature of 50 °C higher than their T_g). An enormous number of stretched PLLA chains may serve as self-nuclei to nucleate their own crystallites. Thus, the PLLA crystals appear discontinuous, with a large number of defects (Fig. 4).

Crystals with different sizes have different melting temperatures (T_ms). The smaller ones with lower T_m melt first as the temperature approaches T_m^{PLLA}. But the larger ones may survive at $T < T_{m,end}^{PLLA}$ [44]. At long time annealing at $T_m^{PLLA} < T < T_{m,end}^{PLLA}$ (e.g., 165 °C), the PLLA chains could adjust their conformation, including refolding of the melted chains into the surviving large crystals. Thus, the crystal structures are improved: the previous defects disappear (Fig. 6) and the melting point of PLLA crystals may increase. The improved PLLA crystals can be partly verified by the increased phase contrast, although the folding plane is likely to be covered by a thin PS layer (hypothesized based on the very small height variation in Fig. 6a and c).

The formation of perpendicular lamellar structure offers additional freedom for the copolymer chains to adjust their conformation since, with comparison to the parallel lamellae, the constraint from the PS chains is largely reduced. Reiter and coworkers reported crystallization-induced formation of perpendicular lamellae in a thin film of a symmetric PEO–PB_h with specific

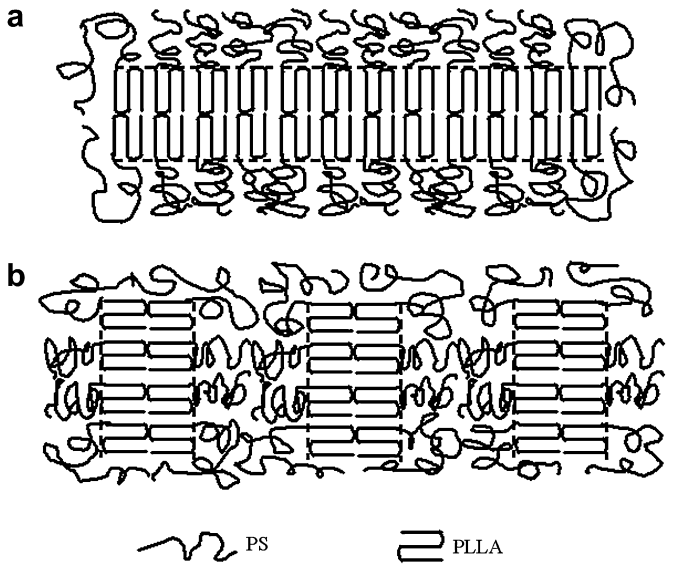

Fig. 7. Schematic drawings of (a) parallel and (b) perpendicular lamellae with crystalline PLLA domains.

composition [38,39]. In melt, the PEO–PB_h formed lamellae parallel to the substrate. As PEO crystallized between rubbery PB_h layers ($T_c \gg T_g^{PBh}$), the lamellae spacing and the interface area per chain decreased, which led to additional interfacial stress. A transition from parallel to perpendicular lamellae took place to relax this stress [33,34]. In our case, the very low phase contrasts may imply the existence of a presumed PS layer on top of the PLLA folding surface, as schematically described in Fig. 7b. Obviously, such perpendicular lamellae allow much more PS chains to relax the repulsion (Fig. 7b) than the parallel lamellae could do since the infinite PS area in parallel lamellae exerts strong lateral confinement on the repulsive PS chains (Fig. 7a). Thus, the perpendicular lamellae are preferable under further crystallization process at higher temperatures, although the lamellae spacing is significantly enhanced (Figs. 4 and 6).

Finally, lets briefly analyze the thickness of PLLA layers after crystallization, with respect to that quenched from melt. At $T_c < T_g^{PS}$, the thickness of PLLA layers (L_{PLLA}), as well as the lamellar spacing, remained unchanged due to the hard confinement from glassy PS phase. At $T_c > T_g^{PS}$, L_{PLLA} increased to 18–25 nm (Figs. 4 and 6), which indicates a decrease in the fold number and an increase in the stem thickness. The length of an unfolded PLLA chain is about 36 nm. There are two possible conformations of the folding chains, assuming that the chains have ideal folding geometry. (1) If the stems are arranged in a zipper-like conformation (Fig. 8a) [39], the PLLA chains are once folded. (2) If the stems follow a so-called cocrystallization mechanism [36], the PLLA chains need to fold three times to make a PLLA layer thickness of 18 nm (Fig. 8b). As the PLLA chains adopt a twice-folded conformation, the PLLA layer will have a thickness of 24 nm (Fig. 8c). These estimations are based on an approximate ignorance of the looping segments, which is usually not negligible.

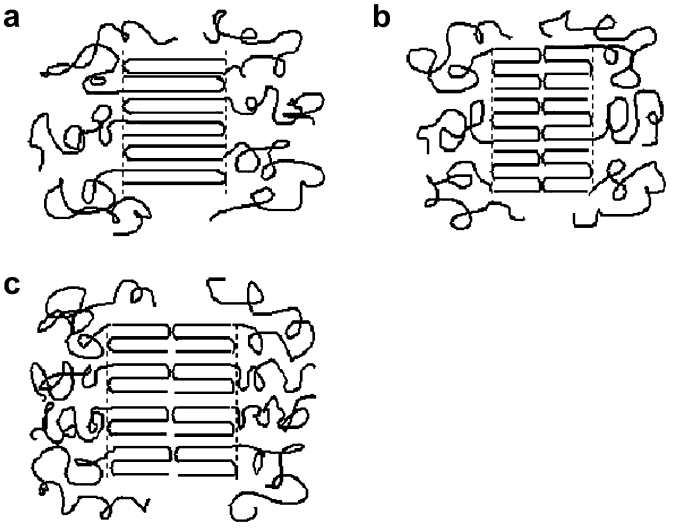

Fig. 8. Possible models for PLLA chain folding. (a) Once-folded zipper model, (b) triple-folded cocrystallization model, and (c) twice-folded cocrystallization model.

Undoubtedly, the zipper model means very narrow interface between the PS and PLLA stems. Thus the PS chains will have strong repulsion with their neighbors and be highly stretched. In contrast, the cocrystallization model has larger interface area and less PS stretching. Therefore, the cocrystallization model might be favorable for the entropy reason, with respect to the zipper model. The stem thickness range between 18 and 25 nm probably implies the possible fold number between two and three for the PLLA chains in confinement (Fig. 8c).

5. Conclusion

The effect of polymer crystallization on the relief structures of the thin films of a symmetric PLLA-*b*-PS diblock copolymer has been investigated by isothermally crystallizing the microphase-separated lamellae films at different temperatures. As the crystallization temperature (T_c) was below T_g^{PS}, the crystallization was strictly confined by the glassy PS walls, without changing the lamellar spacing and the relief pattern. Perpendicular lamellae became into being exclusively at the edge of the islands and holes where local dislocations are believed to nucleate crystals. As $T_g^{PS} < T_c < T_m^{PLLA}$, PLLA crystallization severely cracked the surface relief pattern, and the perpendicular lamellae became popular, especially at the edge of the islands and holes. The lamellar thickness was increased to ~18–25 nm, implying the unfolding of PLLA chains. However, a large number of defects were observed within the PLLA domains. At much higher temperature ($T_m^{PLLA} < T_c < T_{m,end}^{PLLA}$), the PLLA crystallites were melted and recrystallized into larger stems, leading to the formation of well-developed crystals in PLLA layers. Such melting–recrystallization process did not change the lamellae spacing and the PLLA layer thickness, indicating that the PLLA chains may reach some equilibrium fold number between two and three, according to analysis based on a cocrystallization model assumption. However, the actual crystallization and chain conformation inside the PLLA lamellae must be much more complicated than ideal models.

Acknowledgment

The authors are indebted to the financial support from the National Natural Science Foundation of China (20621401, 50573077, and 50773080).

References

[1] Hamley IW. The physics of block copolymers. Oxford: Oxford University Press; 1998.
[2] Bates FS, Fredrickson GH. Ann Rev Phys Chem 1990;41(1):525–57.
[3] Leibler L. Macromolecules 1980;13(6):1602–17.
[4] Rosedale JH, Bates FS, Almdal K, Mortensen K, Wignall GD. Macromolecules 1995;28(5):1429–43.
[5] Green PF, Limary R. Adv Colloid Interface Sci 2001;94(1–3):53–81.

[6] Sakurai S. Polymer 2008;49(12):2781–96.
[7] Hamley IW. Adv Polym Sci 1999;148:25.
[8] Ryan AJ, Hamley IW, Bras W, Bates FS. Macromolecules 1995;28(11):3860–8.
[9] Ho RM, Lin FH, Tsai CC, Lin CC, Ko BT, Hsiao BS, et al. Macromolecules 2004;37(16):5985–94.
[10] Loo Y-L, Register RA, Ryan AJ. Phys Rev Lett 2000;84(18):4120.
[11] Loo YL, Register RA, Ryan AJ, Dee GT. Macromolecules 2001;34(26):8968–77.
[12] Chen HL, Wu JC, Lin TL, Lin JS. Macromolecules 2001;34(20):6936–44.
[13] Quiram DJ, Register RA, Marchand GR, Ryan AJ. Macromolecules 1997;30(26):8338–43.
[14] Hamley IW, Fairclough JPA, Terrill NJ, Ryan AJ, Lipic PM, Bates FS, et al. Macromolecules 1996;29(27):8835–43.
[15] Mai SM, Fairclough JPA, Viras K, Gorry PA, Hamley IW, Ryan AJ, et al. Macromolecules 1997;30(26):8392–400.
[16] Ryan AJ, Fairclough JPA, Hamley IW, Mai SM, Booth C. Macromolecules 1997;30(6):1723–7.
[17] Li L, Serero Y, Koch MHJ, de Jeu WH. Macromolecules 2003;36(3):529–32.
[18] Zhu L, Cheng SZD, Calhoun BH, Ge Q, Quirk RP, Thomas EL, et al. J Am Chem Soc 2000;122(25):5957–67.
[19] Quiram DJ, Register RA, Marchand GR, Adamson DH. Macromolecules 1998;31(15):4891–8.
[20] Huang P, Zhu L, Cheng SZD, Ge Q, Quirk RP, Thomas EL, et al. Macromolecules 2001;34(19):6649–57.
[21] Huang P, Zhu L, Guo Y, Ge Q, Jing AJ, Chen WY, et al. Macromolecules 2004;37(10):3689–98.
[22] Loo YL, Register RA, Adamson DH. Macromolecules 2000;33(22):8361–6.
[23] Loo YL, Register RA, Ryan AJ. Macromolecules 2002;35(6):2365–74.
[24] Ho R-M, Chung T-M, Tsai J-C, Kuo J-C, Hsiao BS, Sics I. Macromol Rapid Commun 2005;26(2):107–11.
[25] Quiram DJ, Register RA, Marchand GR. Macromolecules 1997;30(16):4551–8.
[26] Xu JT, Fairclough JPA, Mai SM, Ryan AJ, Chaibundit C. Macromolecules 2002;35(18):6937–45.
[27] Xu J-T, Fairclough J, Patrick A, Mai S-M, Chaibundit C, Mingvanish M, et al. Polymer 2003;44(22):6843–50.
[28] Chen HL, Li HC, Huang YY, Chiu FC. Macromolecules 2002;35(6):2417–22.
[29] Huang YY, Yang CH, Chen HL, Chiu FC, Lin TL, Liou W. Macromolecules 2004;37(2):486–93.
[30] Hu W. Macromolecules 2005;38(9):3977–83.
[31] Ueda M, Sakurai K, Okamoto S, Lohse DJ, MacKnight WJ, Shinkai S, et al. Polymer 2003;44(22):6995–7005.
[32] Kim G, Han CC, Libera M, Jackson CL. Macromolecules 2001;34(21):7336–42.
[33] Demirel AL, Schlaad H. Polymer 2008;49(16):3470–6.
[34] Coulon G, Russell TP, Deline VR, Green PF. Macromolecules 1989;22(6):2581–9.
[35] Maaloum M, Ausserre D, Chatenay D, Coulon G, Gallot Y. Phys Rev Lett 1992;68(10):1575.
[36] Opitz R, Lambreva DM, de Jeu WH. Macromolecules 2002;35(18):6930–6.
[37] Hong S, MacKnight WJ, Russell TP, Gido SP. Macromolecules 2001;34(9):2876–83.
[38] Reiter G, Castelein G, Hoerner P, Riess G, Blumen A, Sommer J-U. Phys Rev Lett 1999;83(19):3844.
[39] Reiter G, Castelein G, Hoerner P, Riess G, Sommer J-U, Floudas G. Eur Phys J E Soft Matter 2000;2:319–34.
[40] Chen D, Gong Y, He T, Zhang F. Macromolecules 2006;39(12):4101–7.
[41] Chen D, Gong Y, Huang H, He T, Zhang F. Macromolecules 2007;40(18):6631–7.
[42] Zhang F, Chen Y, Huang H, Hu Z, He T. Langmuir 2003;19(14):5563–6.
[43] Zhang F, Huang H, Hu Z, Chen Y, He T. Langmuir 2003;19(24):10100–8.
[44] Fu J, Cong Y, Li J, Luan B, Pan C, Yang Y, et al. Macromolecules 2004;37(18):6918–25.
[45] Fu J, Luan B, Pan C, Li B, Han Y. Macromolecules 2005;38(12):5118–27.
[46] Tao L, Luan B, Pan C-Y. Polymer 2003;44(4):1013–20.
[47] Fu J, Luan B, Yu X, Cong Y, Li J, Pan C, et al. Macromolecules 2004;37(3):976–86.
[48] Zalusky AS, Olayo-Valles R, Wolf JH, Hillmyer MA. J Am Chem Soc 2002;124(43):12761–73.
[49] The term "equilibrium" means the orientation of the lamellae does not change during annealing. But the relief pattern size is subject to change due to ripening.
[50] Note that there is no topography-induced phase contrast between the islands and the valleys although there is a 20-nm fall which is much larger than that between the perpendicular lamellae.
[51] Yuryev Y, Wood-Adams P, Heuzey MC, Dubois C, Brisson J. Polymer 2008;49(9):2306–20.
[52] Liu Y, Rafailovich MH, Sokolov J, Schwarz SA, Bahal S. Macromolecules 1996;29(3):899–906.
[53] Dalvi MC, Lodge TP. Macromolecules 1994;27(13):3487–92.